

TUM-T31-49/93
 hep-ph/9310311
 October 1993

Enhancement of the $K_L - K_S$ Mass Difference by Short Distance QCD Corrections Beyond Leading Logarithms *

Stefan Herrlich [†] and Ulrich Nierste ^{‡§}

Physik-Department T31, Technische Universität München, D-85747 Garching, FRG

Abstract

We calculate the next-to-leading order short distance QCD corrections to the coefficient η_1 of the effective $\Delta S = 2$ hamiltonian in the standard model. This part dominates the short distance contribution $(\Delta m_K)^{\text{SD}}$ to the $K_L - K_S$ mass difference. The next-to-leading order result enhances η_1 and $(\Delta m_K)^{\text{SD}}$ by 20% compared to the leading order estimate. Taking $0.200 \text{ GeV} \leq \Lambda_{\overline{\text{MS}}} \leq 0.350 \text{ GeV}$ and $1.35 \text{ GeV} \leq m_c(m_c) \leq 1.45 \text{ GeV}$ we obtain $0.922 \leq \eta_1^{\text{NLO}} \leq 1.419$ compared to $0.834 \leq \eta_1^{\text{LO}} \leq 1.138$. For $B_K = 0.7$ this corresponds to 48 – 75 % of the experimentally observed mass difference. The inclusion of next-to-leading order corrections to η_1 reduces considerably the theoretical uncertainty related to the choice of renormalization scales.

*Supported by the German Bundesministerium für Forschung und Technologie under the contract 06 TM 732.

[†]e-mail: herrl@feynman.t30.physik.tu-muenchen.de

[‡]e-mail: nierste@feynman.t30.physik.tu-muenchen.de

[§]supported in part by Studienstiftung des Deutschen Volkes

1 Introduction

Over the last three decades the study of the K-meson system has contributed enormously to our insight into the fundamental principles of nature, just to mention the discovery of CP-violation by Christensen et al. [1] and the conjecture of the existence of the charm quark by Glashow, Iliopoulos and Maiani [2]. The latter was derived from the suppression of flavour-changing neutral currents, which is responsible for the smallness of $K^0 - \overline{K}^0$ -mixing. In the following years this $\Delta S = 2$ weak interaction process has been used to investigate the indirect CP-violation apparent in the $K_L - K_S$ mass difference and to constrain the parameters of the Standard Model. The first highlight was clearly the prediction of the mass of the charm quark prior to its discovery by Gaillard and Lee [3].

The theoretical determination of the effective low energy $\Delta S = 2$ -hamiltonian, however, is not satisfactory yet, because the indispensable incorporation of strong interaction effects is difficult due to the poorly known infrared structure of quantum chromodynamics. The theorist's tool to tackle the problem is the use of Wilson's operator product expansion factorizing the Feynman amplitudes into a long distance part, which has to be calculated by non-perturbative methods, and a short distance Wilson coefficient, to which perturbative methods are applicable. The largely separated mass scales in the problem generate large logarithms, whose resummation is mandatory. This is achieved by renormalization group methods applied to a cascade of effective field theories, in which the heavy degrees of freedom are successively removed.

Pioneering work in the short distance calculation of the $\Delta S = 2$ -hamiltonian was done by Vysotskij [4] and by Gilman and Wise [5], who have used the leading logarithmic (LL) approximation. This method leaves certain questions, which will be summarized below, unanswered, and therefore many attempts have been made to include subleading effects.

To be specific, consider the hamiltonian:

$$H^{\Delta S=2}(\mu) = \frac{G_F^2}{16\pi^2} M_W^2 \left[\lambda_c^2 \eta_1 S\left(\frac{m_c^2}{M_W^2}\right) + \lambda_t^2 \eta_2 S\left(\frac{m_t^2}{M_W^2}\right) + 2\lambda_c \lambda_t \eta_3 S\left(\frac{m_c^2}{M_W^2}, \frac{m_t^2}{M_W^2}\right) \right] b(\mu) Q_{LL}(\mu), \quad (1)$$

where G_F is the Fermi constant, $\lambda_j = V_{jd}V_{js}^*$ denotes the CKM-factors, and Q_{LL} is the local four quark operator (see fig. 5 on p. 10)

$$Q_{LL} = (\overline{s}_j \gamma_\mu (1 - \gamma_5) d_j) (\overline{s}_k \gamma^\mu (1 - \gamma_5) d_k) = (\overline{s}d)_{V-A} (\overline{s}d)_{V-A} \quad (2)$$

with j and k being colour indices.

In eq. (1) the GIM mechanism $\lambda_u + \lambda_c + \lambda_t = 0$ has been used to eliminate λ_u . $S(x, y)$ and $S(x)$ denote the Inami-Lim functions [6] resulting from the evaluation of the box diagrams of fig. 1. They must be understood to be expanded to lowest nonvanishing order in m_c^2/M_W^2 in (1).

The η_i 's contain the QCD corrections with their dependence on the renormalization scale μ explicitly factored out in the coefficient $b(\mu)$. In the LL approximation $b(\mu)$ reads in terms of the three-flavour strong interaction constant: $b(\mu) = [\alpha_3(\mu)]^{-2/9}$. In the absence

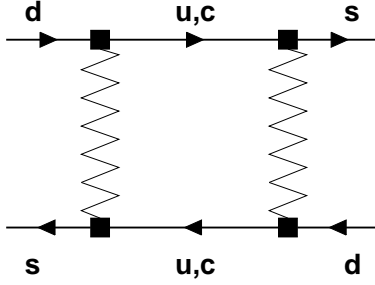


Figure 1: The lowest order box diagrams contributing to $H^{\Delta S=2}$. The zigzag lines stand for W-bosons or fictitious Higgs particles.

of QCD corrections $\eta_i b(\mu) = 1$. Since physical quantities must not depend on μ , $b(\mu)$ has to cancel the corresponding dependence in the matrix element of Q_{LL} , which reads in the case of $K^0 - \bar{K}^0$ -mixing

$$\langle \bar{K}^0 | Q_{LL}(\mu) | K^0 \rangle = \frac{8}{3} B_K(\mu) f_K^2 m_K^2. \quad (3)$$

Here m_K and f_K are the mass and decay constant of the K -meson, and the ‘bag’-parameter $B_K(\mu)$ combines with $b(\mu)$ to the renormalization group invariant

$$B_K = B_K(\mu) b(\mu).$$

In the following we mention the main reasons for going beyond the LL approximation in the calculation of η_1 :

- The running charm quark mass m_c enters $H^{\Delta S=2}$ at the scale $\mu_c \simeq m_c$, at which the effective four-quark theory is matched to an effective three-quark theory. The LL result depends considerably on μ_c .
- Similarly η_1 depends on the scale $\mu_W \simeq M_W$, at which the W-boson is removed from the calculation.
- The definition of the QCD scale parameter Λ requires a next-to-leading order calculation, and therefore one can at most qualitatively discuss the dependence on Λ of physical quantities calculated in the LL approximation.
- After all the subleading terms can be sizeable. The LL hamiltonian only explains about 60 % of the observed $K_L - K_S$ mass difference.

Buras, Jamin and Weisz [7] have improved the result of [5] by including next-to-leading order (NLO) effects into η_2 for $H^{\Delta S=2}$ and $H^{\Delta B=2}$, which, being sensitive to the unknown top-quark mass, is relevant for indirect CP violation in K-decays and $B^0 - \bar{B}^0$ -mixing. They have thoroughly verified that their Wilson coefficient depends neither on the gauge of the gluon propagator nor on the infrared structure of the factorized Feynman amplitude and

proved previous attempts to incorporate NLO effects into $H^{\Delta S=2}$, $H^{\Delta B=2}$ to be incorrect. Since the present work extends theirs to the coefficient η_1 , we closely stick to the notation in [7].

An earlier attempted NLO calculation [9] of η_1 has already been commented on in [7]. The authors of [9] have incorrectly extracted the short distance part of the transition amplitude and have thereby found a drastic decrease in η_1 rather than the sizeable increase found by us.

The coefficient η_1 plays the key role for the $K_L - K_S$ mass difference, while η_2 and η_3 contribute only less than 10%. Since the LL calculation has yielded a too small mass difference, the correction in [9] even worsens the LL result.

The nonperturbative parameter B_K has been calculated using lattice gauge theories [10], $1/N$ expansion [11] and QCD sum rules [12] leading to $B_K = 0.7 \pm 0.2$. The QCD hadron duality approach favours lower values $B_K = 0.4 \pm 0.1$ [13]. For a large N calculation of both short and long distance contributions to the $K_L - K_S$ -mass difference see [14].

Our paper is organized as follows: In section 2 we will set up our notations and present the general outline of the calculations. Section 3 briefly summarizes the LL calculation of [5] changing the assumption $m_t \ll M_W$ into the present day relation $m_t \gtrsim M_W$. Section 4 is devoted to our NLO calculation followed by section 5 containing the numerical analysis of our results. We close the paper by summarizing our main findings.

2 Preliminaries and Conventions

Throughout this paper we work in the $\overline{\text{MS}}$ -scheme using an arbitrary R_ξ -gauge for the gluon propagator and the 't Hooft-Feynman gauge for the W-propagator. Infrared (mass) singularities are regulated by quark masses. Encouraged by [15] and [16] we use an anti-commuting γ_5 (NDR scheme).

The algorithm to perform NLO QCD corrections to weak processes has been outlined in [15, 17, 7], so that we just have to summarize briefly the necessary steps with emphasis on the new features in our calculation.

The part of $H^{\Delta S=2}$ in (1) relevant for η_1 reads

$$H^c(\mu) = \frac{G_F^2}{16\pi^2} M_W^2 \lambda_c^2 \cdot \eta_1(\mu_W, \mu_b, \mu_c) \cdot S\left(\frac{m_c^2(\mu_c)}{M_W^2}\right) \cdot b(\mu) \cdot Q_{LL}(\mu), \quad (4)$$

where we have stressed that the calculation of η_1 involves the scales $\mu_W \simeq M_W$, $\mu_b \simeq m_b$ and $\mu_c \simeq m_c$, at which the W-boson, the bottom and the charm quark are removed from the theory. A physical quantity cannot depend on these scales and any residual dependence of H^c on them is due to the truncation of the perturbation series. To judge the 'theoretical error' associated with this we have varied these scales instead of setting them exactly equal to the values of the corresponding current masses. We will see that the NLO calculation reduces the dependence of the LL result on μ_W , μ_b and μ_c .

2.1 The Hamiltonian at the Scale $\mu_W \simeq M_W$

Consider first the Green's function with the insertion of four weak currents calculated in the full standard model. The lowest order diagrams contributing to it are shown in fig. 1, the $O(\alpha)$ -corrections are displayed in fig. 2.

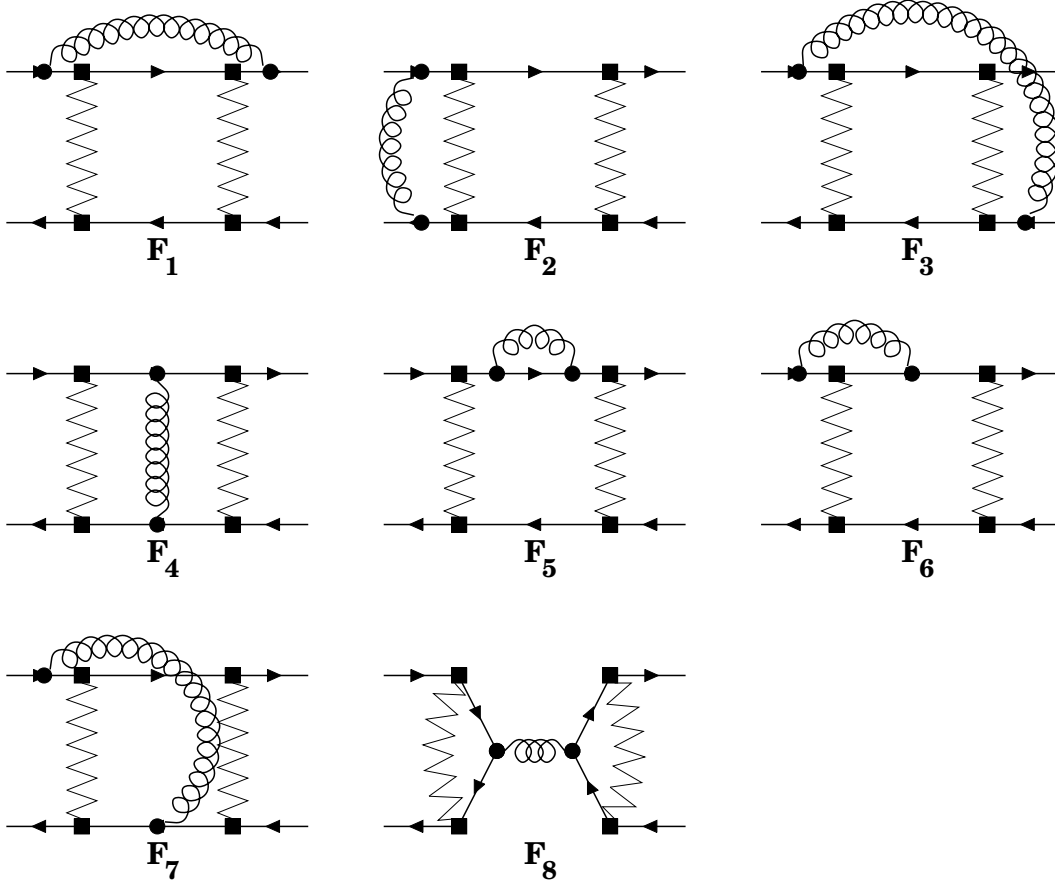


Figure 2: The classes of diagrams contributing to the $O(\alpha)$ -correction to $\langle H^c \rangle$; the remaining diagrams are obtained by left-right and up-down reflections. The curly lines denote gluons. Also QCD counterterm diagrams have to be included. Diagram F_8 evaluates to 0 for zero external momenta.

After multiplication by i they constitute the matrix element of H^c between quark states at the scale $\mu_W \simeq M_W$:

$$\langle H^c(\mu_W) \rangle = \langle H(\mu_W) \rangle^{(0)} + \frac{\alpha(\mu_W)}{4\pi} \langle H(\mu_W) \rangle^{(1)} + O(\alpha^2). \quad (5)$$

In view of the fact that the desired short distance effects do not depend on the treatment of the external states, one can choose free quark states with zero external momenta throughout the whole calculation. The diagrams of fig. 1 with internal quark masses m_i, m_j involve

$\tilde{S}(m_i^2/M_W^2, m_j^2/M_W^2)$ [6, 7], which enter the coefficient of η_1 in the GIM-combination (with $m_u = 0$)

$$\begin{aligned} \tilde{S}\left(\frac{m_c^2}{M_W^2}, \frac{m_c^2}{M_W^2}\right) - 2\tilde{S}\left(\frac{m_c^2}{M_W^2}, \frac{m_u^2}{M_W^2}\right) + \tilde{S}\left(\frac{m_u^2}{M_W^2}, \frac{m_u^2}{M_W^2}\right) &= S\left(\frac{m_c^2}{M_W^2}\right) \\ &= \frac{m_c^2}{M_W^2} + O\left(\frac{m_c^4}{M_W^4}\right) \end{aligned} \quad (6)$$

to give [5]:

$$\langle H(\mu_W) \rangle^{(0)} = \frac{G_F^2}{16\pi^2} \lambda_c^2 m_c^2(\mu_W) \langle Q_{LL} \rangle^{(0)}. \quad (7)$$

The diagrams of fig. 2 have been calculated in [7] giving after inclusion of the GIM mechanism:

$$\langle H(\mu_W) \rangle^{(1)} = \frac{G_F^2}{16\pi^2} \lambda_c^2 m_c^2(\mu_W) \left\{ \langle Q_{LL} \rangle^{(0)} h_{LL}(\mu_W) + \langle \hat{T} \rangle^{(0)} h_T + \langle \hat{U} \rangle^{(0)} h_U \right\}. \quad (8)$$

Only the lowest order in $m_c^2/M_W^2 \ll 1$ has to be kept in (7) and (8).

In (8) new operators have emerged:

$$\begin{aligned} \hat{T} &= (L \otimes L + R \otimes R - \sigma_{\mu\nu} \otimes \sigma^{\mu\nu}) \cdot \frac{N-1}{2N} \hat{1}, \\ \hat{U} &= \frac{1}{2} (\gamma_\mu L \otimes \gamma^\mu R + \gamma_\mu R \otimes \gamma^\mu L) \cdot \left(\frac{N^2 + N - 1}{2N} \hat{1} - \frac{1}{2N} \hat{\bar{1}} \right) \\ &\quad - (L \otimes R + R \otimes L) \cdot \left(\frac{N^2 + N - 1}{2N} \hat{1} - \frac{1}{2N} \hat{\bar{1}} \right), \end{aligned} \quad (9)$$

where $L = 1 - \gamma_5$, $R = 1 + \gamma_5$, N is the number of colours, and $\hat{1}$ and $\hat{\bar{1}}$ denote colour singlet and antisinglet, i.e. $(L \otimes R) \cdot \hat{\bar{1}}$ stands for $\bar{s}_i(1 - \gamma_5)d_j \cdot \bar{s}_j(1 + \gamma_5)d_i$. We have written \hat{U} in a manifestly Fierz self-conjugate way. The Dirac structures of Q_{LL} (see (2)) and \hat{T} are also Fierz self-conjugate.

The functions in (8) are:

$$\begin{aligned} h_{LL}(\mu) &= C_F \left[-1 - 6 \log \frac{m_c^2}{\mu^2} + \xi \left(2 - 2 \frac{m_s^2 \log(m_s^2/\mu^2) - m_d^2 \log(m_d^2/\mu^2)}{m_s^2 - m_d^2} \right) \right] \\ &\quad + \frac{N-1}{2N} \left[-11 + \frac{4}{3} \pi^2 + 12 \log \frac{m_c^2}{M_W^2} + 3 \log \frac{m_d^2 m_s^2}{\mu^4} - 6 \log \frac{m_c^2}{\mu^2} \right. \\ &\quad \left. + \xi \left(2 + \log \frac{m_d^2 m_s^2}{\mu^4} - 2 \frac{m_s^2 \log(m_s^2/\mu^2) - m_d^2 \log(m_d^2/\mu^2)}{m_s^2 - m_d^2} \right) \right] \\ h_T &= (-3 - \xi) \\ h_U &= \frac{3 + \xi}{2} \frac{m_d m_s}{m_s^2 - m_d^2} \log \frac{m_s^2}{m_d^2}, \end{aligned} \quad (10)$$

where $C_F = (N^2 - 1)/(2N)$.

Let us now discuss the structure of $\langle H(\mu_W) \rangle$ in equations (7) to (10): Notice first that there is no large logarithm in (7), the logarithms of the individual box diagrams are cancelled by the GIM mechanism. In h_{LL} in (10) we have arranged the logarithms such that one can easily distinguish those which are small for $\mu \simeq m_c$ from the large logarithm $\log(m_c^2/M_W^2)$. In the LL approximation the terms of the form $[\alpha/(4\pi) \cdot \log(m_c^2/M_W^2)]^n$, $n = 0, 1, 2, \dots$ are summed to all orders in perturbation theory.

Next one observes that $\langle H(\mu_W) \rangle^{(1)}$ involves the additional operators \hat{U} and \hat{T} , which are artefacts of the use of small quark masses m_d and m_s to regulate the mass singularities. Since the desired Wilson coefficient must neither depend on the gauge parameter ξ nor on the infrared regulators, h_U, h_T and the gauge part of h_{LL} must disappear from it, thereby providing a check of the factorization described in section 2.2. Yet in (10) one can see that these terms do not depend on M_W , which sets the scale for the short distance physics.

A dimensional regularization of the mass singularities would have resulted in $h_U = h_T = 0$.

2.2 Factorization of the Hamiltonian at the Scale μ_W

In order to use the renormalization group (RG) evolution to sum the large logarithm $\log(m_c^2/M_W^2)$ to all orders in perturbation theory we seek a factorization of the form

$$H^c \propto \sum_j C_j \mathcal{O}_j \quad (11)$$

with composite operators \mathcal{O}_j describing the weak interaction in an effective field theory without W-boson and top quark. The short distance physics is contained in the Wilson coefficients C_j , to which renormalization group methods will be applied.

Consider first the time ordered product of two weak currents $J_\mu(x)$ folded with the W-propagator $\mathcal{D}^{\mu\nu}$, which mediates a $\Delta S = 1$ transition. Its operator product expansion is well known to order α [18, 15, 17]:

$$-i \int d^4y \mathbf{T} J_\mu^{sj}(x) J_\nu^{kd}(y) \mathcal{D}^{\mu\nu}(x-y) = C_+ Q_+^{jk}(x) + C_- Q_-^{jk}(x) + \dots \quad (12)$$

Here j, k are flavour indices standing for u or c .

$$Q_\pm^{jk} = (\bar{s}j)_{V-A} (\bar{k}d)_{V-A} \cdot \frac{1}{2} \left(\hat{1} \pm \hat{1} \right)$$

are dimension-six four-quark current-current operators, the meaning of $\hat{1}$ and $\hat{\hat{1}}$ has been explained after eq. (9). The dots in (12) denote penguin operators, which contribute to η_3 rather than η_1 , and operators with dimension higher than six.

Now the Green's function described by the diagrams of fig. 1 and 2 contains two insertions of (12) and thus the effective theory involves matrix elements with two insertions of Q_+ or Q_- . In order to find the complete set of operators needed in (11) we have to

look at the forthcoming renormalization group analysis now: The reader may have noticed that we have already put the current–current operators into the basis (Q_+, Q_-) , which is diagonal with respect to the renormalization group evolution. Further the GIM mechanism prevents the mixing under renormalization with penguin operators [17].

For brevity we define the bilocal operators

$$\mathcal{O}_{ij}(x) = \frac{-i}{2} \int d^4y \mathbf{T} \left[Q_i^{cc}(x) Q_j^{cc}(y) + Q_i^{uu}(x) Q_j^{uu}(y) - Q_i^{uc}(x) Q_j^{cu}(y) - Q_i^{cu}(x) Q_j^{uc}(y) \right], \quad i, j = +, - . \quad (13)$$

The diagrams contributing to the matrix element $\langle \mathcal{O}_{ij} \rangle$ are depicted in fig. 3 and 4, the cross denotes the insertion of Q_i or Q_j .

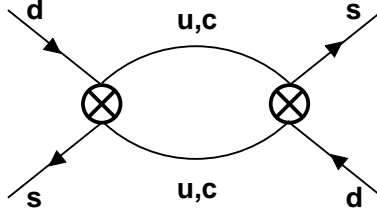


Figure 3: Diagram D_0 in the effective four–quark theory constituting the matrix element of \mathcal{O}_{ij} to order α^0 . The cross denotes the insertion of an effective $\Delta S = 1$ operator.

Now one expects the diagrams of fig. 3 and 4 to be divergent enforcing an extra renormalization of \mathcal{O}_{ij} proportional to a local four–quark operator. The GIM mechanism, however, cancels the divergences. Clearly in fig. 4 one–loop QCD counterterms must be included first. So we end up with

$$H^c(\mu) = \frac{G_F^2}{2} \lambda_c^2 \sum_{i,j=+,-} C_{ij}(\mu) \mathcal{O}_{ij}(\mu). \quad (14)$$

These features have been discovered by Witten [19] a long time before we have carried out this explicit calculation. He has considered four–quark QCD and states:

$$H^c(x) = \frac{-i}{2} \int d^4y \mathbf{T} \left[H^{c,\Delta S=1}(x) H^{c,\Delta S=1}(y) \right],$$

where we have denoted the part of the $\Delta S = 1$ hamiltonian containing the first two quark generations by $H^{c,\Delta S=1}$. For our case this implies that we can simply obtain C_{ij} by multiplying the $\Delta S = 1$ Wilson–coefficients C_i and C_j calculated in [15], where the $\Delta S = 1$ hamiltonian is normalized as

$$H^{\Delta S=1} = \frac{G_F}{\sqrt{2}} \sum_{i=+,-} \sum_{kl} V_{ks}^* V_{ld} C_i Q_i^{kl}.$$

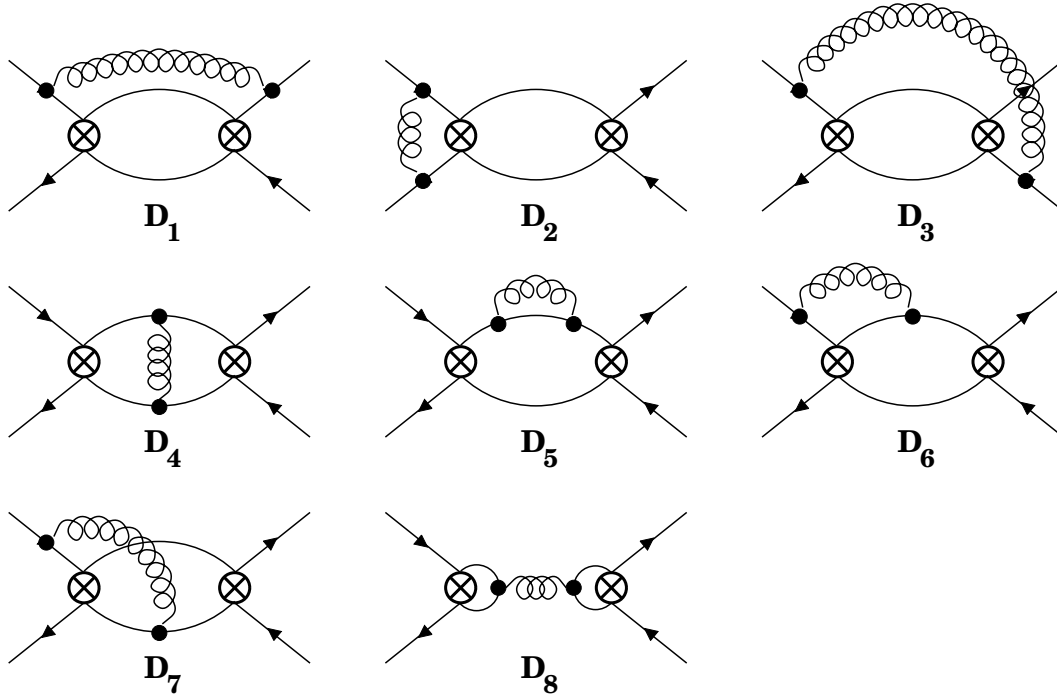


Figure 4: The classes of diagrams in the effective four-quark theory contributing to $O(\alpha)$. The other members of a given class are obtained by left-right and up-down reflections. Also QCD counterterms have to be included. Diagram $D_8 = 0$ for zero external momenta.

This multiplicativity of Wilson coefficients has also been proven for a scalar theory by Lee [20]. Since we anyway need the finite parts of the diagrams of fig. 3 and 4 later in the calculation (section 2.4), we have compared $\sum C_i(\mu_W)C_j(\mu_W)\langle\mathcal{O}_{ij}(\mu_W)\rangle$ with $\langle H^c(\mu_W)\rangle$ as given in eq. (7) and (8) and have indeed verified

$$C_{ij}(\mu_W) = C_i(\mu_W)C_j(\mu_W) \quad (15)$$

to order α .

2.3 Evolution of the Hamiltonian from μ_W to $\mu_c \simeq m_c$

In the next step we want to evolve $C_{ij}(\mu)$ from μ_W down to μ_c using the renormalization group formalism. This procedure is well known [15, 7, 17] and we briefly list its main ingredients:

The running of the coupling constant g ($\alpha = g^2/(4\pi)$) is determined by the beta function

$$\beta(g) = -\beta_0^{(f)} \frac{g^3}{16\pi^2} - \beta_1^{(f)} \frac{g^5}{(16\pi^2)^2} + O(g^7) \quad (16)$$

with f being the number of flavours and

$$\beta_0^{(f)} = \frac{11N - 2f}{3}, \quad \beta_1^{(f)} = \frac{34}{3}N^2 - \frac{10}{3}Nf - 2C_F f. \quad (17)$$

$\alpha(\mu)$ reads in terms of the f-flavour QCD scale parameter Λ_f :

$$\frac{\alpha(\mu)}{4\pi} = \frac{1}{\beta_0^{(f)} \log(\mu^2/\Lambda_f^2)} - \frac{\beta_1^{(f)} \log[\log(\mu^2/\Lambda_f^2)]}{(\beta_0^{(f)})^3 \log^2(\mu^2/\Lambda_f^2)} + O\left(\frac{\log^2[\dots]}{\log^3(\dots)}\right). \quad (18)$$

Λ_3 and Λ_5 are obtained from $\Lambda_4 = \Lambda_{\overline{\text{MS}}}$ by imposing continuity on α .

The anomalous dimension γ_{ij} of \mathcal{O}_{ij} are readily obtained from those of Q_{\pm} via their definition in terms of the renormalization constants Z_{\pm} . Since no matrix renormalization is required for Q_{\pm} and the bilocal operators \mathcal{O}_{ij} do not mix with local operators, also \mathcal{O}_{ij} renormalizes multiplicatively, so that

$$\gamma_{ij} = (Z_i Z_j)^{-1} \mu \frac{d}{d\mu} (Z_i Z_j) = \gamma_i + \gamma_j, \quad i, j = +, -.$$

The coefficients $\gamma_{\pm}^{(0)}$ and $\gamma_{\pm}^{(1)(f)}$ of the anomalous dimension of Q_{\pm} ,

$$\gamma_{\pm}(g) = \gamma_{\pm}^{(0)} \frac{g^2}{16\pi^2} + \gamma_{\pm}^{(1)(f)} \left(\frac{g^2}{16\pi^2}\right)^2 + O(g^6),$$

read in the NDR scheme [15]:

$$\gamma_{\pm}^{(0)} = \pm 6 \frac{N \mp 1}{N}, \quad \gamma_{\pm}^{(1)(f)} = \frac{N \mp 1}{2N} \left(-21 \pm \frac{57}{N} \mp \frac{19}{3} N \pm \frac{4}{3} f\right). \quad (19)$$

We define for $i, j = +, -$:

$$\begin{aligned} d_j^{(f)} &= \frac{\gamma_j^{(0)}}{2\beta_0^{(f)}}, & d_{ij}^{(f)} &= d_i^{(f)} + d_j^{(f)}, \\ Z_j^{(f)} &= \frac{\gamma_j^{(1)} - 2\beta_1^{(f)} d_j^{(f)}}{2\beta_0^{(f)}}, & Z_{ij}^{(f)} &= Z_i^{(f)} + Z_j^{(f)}, \end{aligned} \quad (20)$$

so that the solution to the renormalization group equation for $C_{ij}(\mu)$ reads below the b-quark threshold μ_b in NLO:

$$\begin{aligned} C_{ij}(\mu) &= C_{ij}(\mu_W) \left(\frac{\alpha(\mu_W)}{\alpha(\mu_b)}\right)^{d_{ij}^{(5)}} \left(\frac{\alpha(\mu_b)}{\alpha(\mu)}\right)^{d_{ij}^{(4)}} \\ &\quad \left(1 + \frac{\alpha(\mu_W) - \alpha(\mu_b)}{4\pi} Z_{ij}^{(5)} + \frac{\alpha(\mu_b) - \alpha(\mu)}{4\pi} Z_{ij}^{(4)}\right) \\ &= C_i(\mu) C_j(\mu). \end{aligned} \quad (21)$$

Hence the RG improved Wilson coefficient C_{ij} also equals $C_i \cdot C_j$.

2.4 The Hamiltonian below μ_c

Below the scale $\mu_c \simeq m_c$ the c -quark field is no more a dynamic degree of freedom and we have to express $H^c(\mu)$ in an effective three-quark theory. Here we are left with the single local four-quark operator Q_{LL} defined in eq. (2).

To obtain the Wilson coefficient C in

$$H^c(\mu) = \frac{G_F^2}{16\pi^2} \lambda_c^2 C(\mu) Q_{LL}(\mu) \quad (22)$$

one must first solve the matching condition between the four- and three-quark theory:

$$\frac{G_F^2}{2} \lambda_c^2 \sum_{i,j=+,-} C_{ij}(\mu_c) \langle \mathcal{O}_{ij}(\mu_c) \rangle = \frac{G_F^2}{16\pi^2} \lambda_c^2 C(\mu_c) \langle Q_{LL}(\mu_c) \rangle. \quad (23)$$

At this stage the matrix elements $\langle \mathcal{O}_{ij} \rangle$ must be calculated. $\langle Q_{LL} \rangle$ has already been obtained to order α in [7]. The corresponding diagrams are depicted in fig. 5 and 6.

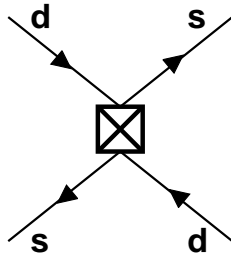


Figure 5: The diagram for the matrix element of Q_{LL} in the effective three-quark theory to order α^0 . The cross denotes the insertion of the effective $\Delta S = 2$ operator.

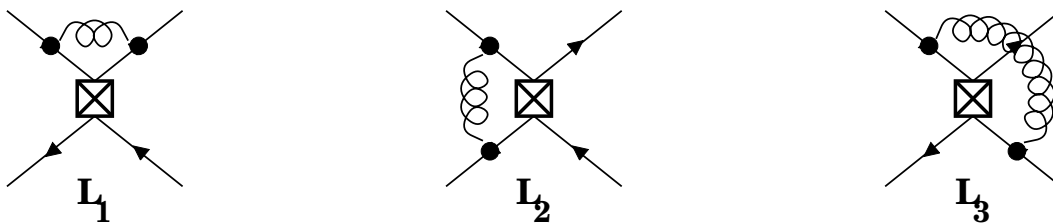


Figure 6: Classes of diagrams in the effective three-quark theory contributing to $\langle Q_{LL} \rangle$ to order α . The other members of a given class are obtained by left-right and up-down reflections. QCD counterterms have to be included.

Since the LL analysis sums up the terms $[\alpha \cdot \text{large log}]^n$ for $n = 0, 1, 2, \dots$, to all orders in perturbation theory, the LL matching has to be made to order α^0 . Consequently in NLO the terms $\alpha [\alpha \cdot \text{large log}]^n$, $n = 0, 1, 2, \dots$, are summed, and one has to match the

effective theories to order α^1 . For this the finite parts of the diagrams of fig. 4 must be calculated.

This is in contrast to the recent NLO analysis of $K^+ \rightarrow \pi^+ \nu \bar{\nu}$, $K_L \rightarrow \mu^+ \mu^-$ by Buchalla and Buras [21], which also involves the renormalization of bilocal operators. There the one-loop Green's function already contains a large logarithm and therefore the NLO matching can be made at the one-loop level.

The evolution of $C(\mu)$ in (22) to scales below μ_c is dictated by the anomalous dimension of Q_{LL} , which equals γ_+ in (19) [15]:

$$C(\mu) = C(\mu_c) \left(\frac{\alpha(\mu_c)}{\alpha(\mu)} \right)^{d_+^{(3)}} \left(1 + \frac{\alpha(\mu_c) - \alpha(\mu)}{4\pi} Z_+^{(3)} + O(\alpha^2) \right). \quad (24)$$

The residual μ -dependence in (24) is absorbed into $b(\mu)$ defined in (1):

$$b(\mu) = [\alpha(\mu)]^{-d_+^{(3)}} \left(1 - \frac{\alpha(\mu)}{4\pi} Z_+^{(3)} + O(\alpha^2) \right). \quad (25)$$

We close this section by noting that $C(\mu)$ has via (23) absorbed all dependence on the charm quark mass present in $\langle \mathcal{O}_{ij}(\mu_c) \rangle$, because the matrix element $\langle Q_{LL}(\mu_c) \rangle$ is evaluated in an effective three-quark theory containing no information on m_c . Consequently $C(\mu)$ contains the running charm quark mass in the form $m_c(\mu_c)$.

To discuss the dependence of our result on the scale μ_c in section 5, we need the anomalous mass dimension γ_m , which is given by

$$\gamma_m(g) = \gamma_m^{(0)} \frac{g^2}{16\pi^2} + \gamma_m^{(1)(f)} \left(\frac{g^2}{16\pi^2} \right)^2 + O(g^6)$$

with

$$\gamma_m^{(0)} = 6C_F, \quad \gamma_m^{(1)(f)} = C_F \left(3C_F + \frac{97}{3}N - \frac{10}{3}f \right). \quad (26)$$

Hence with

$$d_m^{(f)} = \frac{\gamma_m^{(0)}}{2\beta_0^{(f)}} \quad \text{and} \quad Z_m^{(f)} = \frac{\gamma_m^{(1)(f)} - 2\beta_1^{(f)} d_m^{(f)}}{2\beta_0^{(f)}}$$

the running mass reads

$$m_c(\mu_c) = m_c(m_c) \left(\frac{\alpha(\mu_c)}{\alpha(m_c)} \right)^{d_m^{(f)}} \left(1 + \frac{\alpha(\mu_c) - \alpha(m_c)}{4\pi} Z_m^{(f)} \right). \quad (27)$$

3 The Leading Log Analysis

In this section we review the LL analysis of [5] using the formalism of section 2 and taking into account that the top quark is heavy. This analysis has already been performed by Flynn [22]. A good approximation neglecting quark thresholds has been given by Datta, Fröhlich and Paschos [23]. We discuss the scale dependences inherent to the LL calculation. The relevant RG formulae are obtained from those in section 2 by setting $\beta_1^{(f)}$, $\gamma_{\pm}^{(1)(f)}$ and $\gamma_m^{(1)(f)}$ to zero.

3.1 The Hamiltonian between the Scales μ_c and μ_W

At first we want to factorize the $H^c(\mu)$ for $\mu_c \leq \mu \leq \mu_W$ in order to separate short and long distance physics as described in sections 2.2 and 2.3:

$$\langle H^c(\mu) \rangle = \frac{G_F^2 \lambda_c^2}{2} \sum_{i,j=+,-} C_{ij}(\mu) \langle \mathcal{O}_{ij}(\mu) \rangle^{(0)}. \quad (28)$$

At the matching scale μ_W the left hand side of (28) simply equals $\langle H^c(\mu_W) \rangle^{(0)}$ given in (7). The $\Delta S = 1$ Wilson coefficients $C_{\pm}(\mu_W)$ are equal to 1 in the LL approximation [15, 24], so that we get $C_{ij}(\mu_W) = 1$ by means of (15).

In section 3.2 we will need (see fig. 3)

$$\langle \mathcal{O}_{ij}(\mu) \rangle^{(0)} = \tau_{ij} \frac{m_c^2(\mu)}{8\pi^2} \langle Q_{LL} \rangle^{(0)} \quad (29)$$

with

$$\tau_{++} = \frac{N+3}{4}, \quad \tau_{+-} = \tau_{-+} = \frac{-N+1}{4}, \quad \tau_{--} = \frac{N-1}{4}.$$

Using (29) and (7) one easily checks (28).

$\langle H^c(\mu_W) \rangle$ contains the Inami–Lim function S , which has been expanded to lowest order in m_c^2/M_W^2 in (6). To include higher order terms, $(m_c^2/M_W^2)^2 \dots$ in the factorization (28), one must take into account operators with dimension higher than six in (12).

Next we seek the resummation of the large logarithm $\alpha \log(m_c^2/M_W^2)$ present in the higher order terms of H^c . The factorization (28) splits $\log(m_c^2/M_W^2)$ into $\log(\mu^2/M_W^2) + \log(m_c^2/\mu^2)$. While the latter resides in the matrix elements, the former is contained in the Wilson coefficients and is summed to all orders by the renormalization group evolution from μ_W to μ_c .

The LL running of the Wilson coefficients down to μ_c is given by

$$C_{ij}(\mu_c) = \left(\frac{\alpha(\mu_b)}{\alpha(\mu_c)} \right)^{d_{ij}^{(4)}} \left(\frac{\alpha(\mu_W)}{\alpha(\mu_b)} \right)^{d_{ij}^{(5)}} C_{ij}(\mu_W), \quad (30)$$

where d_{ij} has been defined in (20), and the LL running for α must be used.

Now we show the effect of the RG resummation on (28). Setting $\mu_W = M_W$, $\mu_c = m_c$ for the moment and expanding (30) around M_W to order $\alpha \log(m_c^2/M_W^2)$ yields with (29):

$$\langle H^c(m_c) \rangle = \frac{G_F^2}{16\pi^2} \lambda_c^2 m_c^2(m_c) \langle Q_{LL} \rangle^{(0)} \cdot \left[1 + \frac{\alpha}{4\pi} \log\left(\frac{m_c^2}{M_W^2}\right) \sum_{i,j=+,-} \frac{\gamma_{ij}^{(0)}}{2} \tau_{ij} + O\left(\alpha^2 \log^2\left(\frac{m_c^2}{M_W^2}\right)\right) \right]. \quad (31)$$

Since $\sum \tau_{ij} \gamma_{ij}^{(0)}/2 = 12(N-1)/(2N)$, we have reproduced in (31) the large logarithm present in the coefficient h_{LL} of (8).

3.2 The Hamiltonian below the Scale μ_c

At the scale μ_c we obtain $C(\mu_c)$ from the matching condition (23):

$$C(\mu_c) = m_c^2(\mu_c) \sum_{i,j=+,-} \tau_{ij} \left(\frac{\alpha(\mu_b)}{\alpha(\mu_c)}\right)^{d_{ij}^{(4)}} \left(\frac{\alpha(\mu_W)}{\alpha(\mu_b)}\right)^{d_{ij}^{(5)}}. \quad (32)$$

The LL evolution of $C(\mu)$ below μ_c can be obtained from the corresponding NLO expression in (24) by setting $Z_+^{(3)}$ to zero.

Hence η_1 as defined in (1) or (4) reads in the LL approximation:

$$\begin{aligned} \eta_1^{\text{LO}} &= (\alpha(\mu_c))^{d_+^{(3)}} \sum_{i,j=+,-} \tau_{ij} \left(\frac{\alpha(\mu_b)}{\alpha(\mu_c)}\right)^{d_{ij}^{(4)}} \left(\frac{\alpha(\mu_W)}{\alpha(\mu_b)}\right)^{d_{ij}^{(5)}} \\ &= (\alpha(\mu_c))^{2/9} \left[\frac{3}{2} \left(\frac{\alpha(\mu_b)}{\alpha(\mu_c)}\right)^{12/25} \left(\frac{\alpha(\mu_W)}{\alpha(\mu_b)}\right)^{12/23} - \left(\frac{\alpha(\mu_b)}{\alpha(\mu_c)}\right)^{-6/25} \left(\frac{\alpha(\mu_W)}{\alpha(\mu_b)}\right)^{-6/23} \right. \\ &\quad \left. + \frac{1}{2} \left(\frac{\alpha(\mu_b)}{\alpha(\mu_c)}\right)^{-24/25} \left(\frac{\alpha(\mu_W)}{\alpha(\mu_b)}\right)^{-24/23} \right]. \end{aligned} \quad (33)$$

In the preceding sketch of the LL calculation we have seen how the various scales μ_W , μ_b and μ_c enter the result of η_1^{LO} . H^c , which is related to physical observables, must not depend on these scales, and we can vary them in (33) to judge the accuracy of the perturbative calculation. The residual scale dependence of (33) is sizeable and is substantially reduced in the NLO result. A comparative numerical analysis of the LL and NLO scale setting ambiguity will be postponed until section 5, and at this place we just display the sources of the scale dependence analytically.

The coupling constant grows with decreasing scale, H^c is therefore most sensitive to the variation of the smallest scale μ_c , and we exemplify the scale dependence by expanding the concerning parts of the hamiltonian around $m_c^* = m_c(m_c)$. They read

$$\eta_1^{\text{LO}}(\mu_c) m_c^2(\mu_c) = (m_c^*)^2 (\alpha(m_c^*))^{d_+^{(3)}} \sum_{i,j=+,-} \left(\frac{\alpha(\mu_b)}{\alpha(m_c^*)}\right)^{d_{ij}^{(4)}} \left(\frac{\alpha(\mu_W)}{\alpha(\mu_b)}\right)^{d_{ij}^{(5)}}.$$

$$\tau_{ij} \left[1 + \frac{\alpha}{4\pi} \log \frac{\mu_c^2}{(m_c^*)^2} \left(\frac{\gamma_{ij}^{(0)} - \gamma_+^{(0)}}{2} - \gamma_m^{(0)} \right) + O \left(\alpha^2 \log^2 \frac{\mu_c^2}{(m_c^*)^2} \right) \right]. \quad (34)$$

Notice that the largest contribution to the coefficient of $\alpha \log(\mu_c^2/m_c^2)$ comes from the anomalous dimension of \mathcal{O}_{--} . The two-loop finite part of the NLO analysis will encounter a term which cancels the logarithm in (34) and will thereby diminish the scale ambiguity.

4 The Next-to-Leading Order Analysis

In this section we describe in detail our NLO calculation, in which the $O(\alpha)$ -contribution to the transition amplitude (fig. 2) is improved by summing the terms $\alpha^{n+1} \log^n(m_c^2/M_W^2)$, $n = 0, 1, 2, \dots$, to all orders in perturbation theory.

4.1 The Hamiltonian between the Scales μ_c and μ_W

For the NLO factorization

$$\langle H^c(\mu) \rangle = \frac{G_F^2}{2} \lambda_c^2 \sum_{i,j=+,-} C_{ij}(\mu) \langle \mathcal{O}_{ij}(\mu) \rangle, \quad \mu_c \leq \mu \leq \mu_W, \quad (35)$$

we need the $\Delta S = 1$ Wilson coefficients C_{\pm} to order α . At the matching point one has [15]:

$$C_{\pm}(\mu_W) = 1 + \frac{\alpha(\mu_W)}{4\pi} \left(\frac{\gamma_{\pm}^{(0)}}{2} \log \frac{\mu_W^2}{M_W^2} + B_{\pm} \right) + O(\alpha^2) \quad (36)$$

with B_{\pm} given in the NDR scheme

$$B_{\pm} = \pm 11 \frac{N \mp 1}{2N}. \quad (37)$$

Hence in (35)

$$C_{ij}(\mu_W) = 1 + \frac{\alpha(\mu_W)}{4\pi} \left(\frac{\gamma_{ij}^{(0)}}{2} \log \frac{\mu_W^2}{M_W^2} + B_i + B_j \right) + O(\alpha^2). \quad (38)$$

As outlined in section 2.1 the factorization (35) is so simple because of the absence of mixing between \mathcal{O}_{ij} and local operators. Let us briefly explain why they do not mix: The diagrams of fig. 3 and 4 contain two internal quarks with masses m_k and m_l , each of which is m_u or m_c . The elements of the anomalous dimension matrix responsible for the mixing can directly be read off from the divergent parts of these diagrams. Since the diagrams have dimension 2 and the anomalous dimension does not depend explicitly on μ in a mass independent renormalization scheme as $\overline{\text{MS}}$, the singular part of the diagrams must be proportional to $m_k^2 + m_l^2$ by symmetry under $m_k \leftrightarrow m_l$. Hence in the GIM-combination

$(k, l) = (c, c) - 2(c, u) + (u, u)$ the divergent parts cancel and no mixing with local operators occurs.

Since we had to calculate the two-loop contributions to $\langle \mathcal{O}_{ij} \rangle$ shown in fig. 4 for the matching at μ_c described in section 4.2, we could verify (35) and analyze the contributions of the individual diagrams to C_{ij} : The diagrams D₂, D₄, D₆ and D₇ contain each one tree-level and one dressed $\Delta S = 1$ four-quark operator as subdiagrams. All other diagrams can be divided by a three-particle cut through the gluon line and the u/c -quark lines into two subdiagrams, each of which contains a tree-level $\Delta S = 1$ operator with four (anti-)quarks and one gluon as external states. In (35) the latter match their corresponding counterparts of fig. 2 with the tree-level Wilson coefficient, thus these diagrams are also properly taken into account in (35). Hence there is no point in treating the diagrams D₁, D₃, D₄ and D₅ differently from the others as done by the authors of [9]. In fact only D₂, D₄ and D₇ contribute to the $O(\alpha)$ -part in (36). D₆ contains a dressed colour singlet $\Delta S = 1$ operator, which does not contribute to the $O(\alpha)$ -part of C_{\pm} [15], and therefore matches the diagram F₆ with the tree-level Wilson coefficient. Finally the term with $\log(\mu_W^2/M_W^2)$ in (36) originates solely from D₇. We will see in a moment that this term will reduce the dependence of C_{ij} on μ_W .

The RG improved Wilson coefficient at μ_c is immediately obtained from (21) and (38):

$$C_{ij}(\mu_c) = \left(\frac{\alpha(\mu_b)}{\alpha(\mu_c)} \right)^{d_{ij}^{(4)}} \left(\frac{\alpha(\mu_W)}{\alpha(\mu_b)} \right)^{d_{ij}^{(5)}} \left[1 + \frac{\alpha(\mu_b) - \alpha(\mu_c)}{4\pi} Z_{ij}^{(4)} + \frac{\alpha(\mu_W) - \alpha(\mu_b)}{4\pi} Z_{ij}^{(5)} + \frac{\alpha(\mu_W)}{4\pi} \left(\frac{\gamma_{ij}^{(0)}}{2} \log \frac{\mu_W^2}{M_W^2} + B_i + B_j \right) \right]. \quad (39)$$

We close this section by noting that in (39) the LL scale ambiguity at μ_W is removed to order α due to

$$[\alpha(\mu_W)]^{d_{ij}^{(5)}} \left(1 + \frac{\alpha(\mu_W)}{4\pi} \frac{\gamma_{ij}^{(0)}}{2} \log \frac{\mu_W^2}{M_W^2} \right) = [\alpha(M_W)]^{d_{ij}^{(5)}} + O(\alpha^2).$$

4.2 The Hamiltonian below the Scale μ_c

To obtain the hamiltonian for $\mu \leq \mu_c$ given in (22) we must first solve the matching condition between the three- and four-quark theory for $C(\mu)$:

$$\langle H^c(\mu_c) \rangle = \frac{G_F^2}{2} \lambda_c^2 \sum_{i,j=+,-} C_{ij}(\mu_c) \langle \mathcal{O}_{ij}(\mu_c) \rangle = \frac{G_F^2}{16\pi^2} \lambda_c^2 C(\mu_c) \langle Q_{LL}(\mu_c) \rangle. \quad (40)$$

As discussed in section 2.4 this step requires the calculation of the finite parts of the two-loop diagrams shown in fig. 4.

4.2.1 Calculation of the Two-Loop Diagrams in Fig. 4

We now sketch some details of the two-loop calculation, which has been carried out independently by both of us.

The diagrams of fig. 4 in arbitrary R_ξ -gauge for the gluon involve tensor integrals up to rank six. As explained in section 2.1 we could set the external momenta to zero, the masses $m_{k,l}$ of the internal quark lines connecting the four-quark operators were kept arbitrary and in the very end set equal to m_c or to $m_u = 0$. Diagrams D_1 through D_3 are infrared singular and we have kept nonzero strange and down quark masses for their regularization. Alternatively one could use an off-shell external momentum or regulate both UV- and IR-singularities dimensionally. Needless to say that the same regularization must be used for all matrix elements in (40). It turned out to be convenient to calculate the integrals keeping the space-time dimension D arbitrary, which has resulted in quite compact expressions for the coefficients of the various tensors built out of combinations of metric tensors. These coefficients involve Gauß' hypergeometric function ${}_2F_1$, whose expansion in terms of $\varepsilon = (4-D)/2$ yields quite lengthy expressions containing the familiar dilogarithm function in the finite part. D_1 , D_2 and D_3 also contain additive terms with the IR-regulators. The dilogarithms disappear for $m_k = m_l = m_c$ or $m_{k,l} = m_u \rightarrow 0$. Only a few number of the hypergeometric functions must be expanded explicitly, the others can be obtained via functional equations. As a byproduct we have obtained the results corresponding to a dimensional infrared regularization. The $1/\varepsilon^2$ -terms of the diagrams disappear in the GIM-combination.

The D -dimensional Dirac algebra has been evaluated with the help of the package TRACER [25] for the computer algebra system MATHEMATICA. The results involve products of up to five Dirac matrices on each fermion line. They have to be projected onto a set of Dirac structures which form a basis for $D = 4$. We have chosen the following convention:

$$\begin{aligned}\gamma_\mu\gamma_\nu\gamma_\vartheta L \otimes \gamma^\mu\gamma^\nu\gamma^\vartheta L &= (16 - 4\varepsilon)\gamma_\nu L \otimes \gamma^\nu L + \text{ev.} \\ \gamma_\rho\gamma_\delta\gamma_\mu\gamma_\nu\gamma_\vartheta L \otimes \gamma^\rho\gamma^\delta\gamma^\mu\gamma^\nu\gamma^\vartheta L &= (256 - 224\varepsilon)\gamma_\nu L \otimes \gamma^\nu L + \text{ev.}\end{aligned}\quad (41)$$

where $L = 1 - \gamma_5$ and ev. stands for evanescent operators vanishing for $D = 4$. The infrared singular diagrams contain additional Dirac structures, which multiply only finite integrals.

The same procedure has to be performed for the graphs with QCD counterterms for the inserted $\Delta S = 1$ operators. The diagrams of fig. 4 also contain divergent subloops involving both $\Delta S = 1$ operators, their divergent parts vanish in the GIM-combination like the divergence of fig. 3, so that no counterterms for these subdivergences are needed.

After summing the diagrams we indeed verify that the divergences disappear by GIM as stated in section 4.1. We remark that the evanescent operators in (41) can in general mix into physical operators [15]. We have checked that this is not the case here.

The results for the individual diagrams of fig. 3 and 4 can be found in the appendix. They represent

$$\langle \mathcal{O}_{ij}(\mu) \rangle = \langle \mathcal{O}_{ij}(\mu) \rangle^{(0)} + \frac{\alpha(\mu)}{4\pi} \langle \mathcal{O}_{ij}(\mu) \rangle^{(1)} + O(\alpha^2)$$

with $\langle \mathcal{O}_{ij}(\mu) \rangle^{(0)}$ given in (29) and

$$\langle \mathcal{O}_{ij}(\mu) \rangle^{(1)} = \frac{m_c^2(\mu)}{8\pi^2} \left[\langle Q_{LL} \rangle^{(0)} a_{LL}^{(ij)}(\mu) + \langle \hat{T} \rangle^{(0)} \tau_{ij} h_T + \langle \hat{U} \rangle^{(0)} \tau_{ij} h_U \right]. \quad (42)$$

Let us analyze (42) first by looking back at the factorization at $\mu = \mu_W$: The unphysical Dirac structures \hat{T} and \hat{U} come with the same coefficient functions h_T and h_U defined in (10) as $\langle H(\mu_W) \rangle^{(1)}$ in (8). τ_{ij} has been defined in (29), and with $\sum \tau_{ij} = 1$ the factorization of the \hat{T} - and \hat{U} -part at $\mu = \mu_W$ becomes transparent in (35). We split $a_{LL}^{(ij)}$ in (42) into its physical part $c_{LL}^{(ij)}$ and those parts which depend on the infrared regulators or involve the gauge parameter:

$$\begin{aligned} a_{LL}^{(ij)}(\mu) = & c_{LL}^{(ij)}(\mu) + \tau_{ij} \left\{ \frac{N-1}{2N} 3 \log \frac{m_d^2 m_s^2}{\mu^4} \right. \\ & + \xi \left[\left(C_F + \frac{N-1}{2N} \right) \left(2 - 2 \frac{m_s^2 \log(m_s^2/\mu^2) - m_d^2 \log(m_d^2/\mu^2)}{m_s^2 - m_d^2} \right) \right. \\ & \left. \left. + \frac{N-1}{2N} \log \frac{m_d^2 m_s^2}{\mu^4} \right] \right\}. \end{aligned} \quad (43)$$

Clearly also in (43) the unphysical terms coincide with those of (10), so that they correctly give no contribution in (35) to the Wilson coefficient.

The desired physical parts in (43) read:

$$\begin{aligned} c_{LL}^{(++)}(\mu) = & \tau_{++} 3(1-N) \log \frac{m_c^2(\mu)}{\mu^2} \\ & + \frac{102 - 73N - 32N^2 + 3N^3}{8N} + \pi^2 \frac{-6 + 6N + N^2 - N^3}{12N}, \\ c_{LL}^{(+-)}(\mu) = c_{LL}^{(-+)}(\mu) = & \tau_{+-} 3(-1-N) \log \frac{m_c^2(\mu)}{\mu^2} \\ & + \frac{34 - 39N + 8N^2 - 3N^3}{8N} + \pi^2 \frac{-2 + 4N - 3N^2 + N^3}{12N}, \\ c_{LL}^{(--) }(\mu) = & \tau_{--} 3(-3-N) \log \frac{m_c^2(\mu)}{\mu^2} \\ & + \frac{-34 + 19N + 12N^2 + 3N^3}{8N} + \pi^2 \frac{2 - 6N + 5N^2 - N^3}{12N}. \end{aligned} \quad (44)$$

With (44) one verifies (35) as promised in section 4.1.

4.2.2 Determination of the Wilson Coefficient $C(\mu)$

Next we want to use (42) to solve (40) for $C(\mu_c)$. To this end we also need $\langle Q_{LL} \rangle$, which is made up of the diagrams of fig. 5 and 6. One has [15]

$$\langle Q_{LL}(\mu) \rangle = \langle Q_{LL}(\mu) \rangle^{(0)} + \frac{\alpha(\mu)}{4\pi} \left[\langle Q_{LL} \rangle^{(0)} a(\mu) + \langle \hat{T} \rangle^{(0)} h_T + \langle \hat{U} \rangle^{(0)} h_U \right]. \quad (45)$$

Here h_T and h_U have been defined in (10), and we extract the physical part c out of $a(\mu)$:

$$\begin{aligned}
a(\mu) &= c + \left\{ \frac{N-1}{2N} 3 \log \frac{m_d^2 m_s^2}{\mu^4} \right. \\
&\quad \left. + \xi \left[\left(C_F + \frac{N-1}{2N} \right) \left(2 - 2 \frac{m_s^2 \log(m_s^2/\mu^2) - m_d^2 \log(m_d^2/\mu^2)}{m_s^2 - m_d^2} \right) \right. \right. \\
&\quad \left. \left. + \frac{N-1}{2N} \log \frac{m_d^2 m_s^2}{\mu^4} \right] \right\}, \\
c &= -3C_F - 5 \frac{N-1}{2N}.
\end{aligned} \tag{46}$$

Now we are in a position to solve the matching condition (40) for $C(\mu_c)$:

$$\begin{aligned}
C(\mu_c) &= m_c^2(\mu_c) \sum_{i,j=+,-} \left(\frac{\alpha(\mu_b)}{\alpha(\mu_c)} \right)^{d_{ij}^{(4)}} \left(\frac{\alpha(\mu_W)}{\alpha(\mu_b)} \right)^{d_{ij}^{(5)}} \left\{ \tau_{ij} \left[1 + \frac{\alpha(\mu_b) - \alpha(\mu_c)}{4\pi} Z_{ij}^{(4)} \right. \right. \\
&\quad \left. \left. + \frac{\alpha(\mu_W) - \alpha(\mu_b)}{4\pi} Z_{ij}^{(5)} + \frac{\alpha(\mu_W)}{4\pi} b_{ij}(\mu_W) \right] + \frac{\alpha(\mu_c)}{4\pi} r_{ij}(\mu_c) \right\}.
\end{aligned} \tag{47}$$

Here

$$b_{ij}(\mu_W) = \frac{\gamma_{ij}^{(0)}}{2} \log \frac{\mu_W^2}{M_W^2} + B_i + B_j, \quad i, j = +, -, \tag{48}$$

where B_{\pm} defined in (37) originates from the matching at μ_W , while τ_{ij} and

$$r_{ij}(\mu_c) = c_{LL}^{ij}(\mu_c) - \tau_{ij}c \tag{49}$$

have entered the result at the c-quark threshold μ_c . All other quantities in (47) are related to the RG evolution.

Notice that again those parts of $\langle \mathcal{O}_{ij} \rangle$ and $\langle Q_{LL} \rangle$ which depend on the IR structure or the gauge parameter have not contributed to the Wilson coefficient. By working in an arbitrary R_{ξ} -gauge for the gluon we have explicitly proven that our final Wilson coefficient $C(\mu)$ is gauge independent. The use of small quark masses m_s and m_d as infrared regulators has enabled us to verify that $C(\mu)$ does not depend on the infrared structure. This would not have been so, if we had regulated both UV and IR singularities dimensionally, because the infrared structure would not have been explicit and the factorizations would have been trivial due to the absence of the operators \hat{T} and \hat{U} .

$C(\mu)$ for $\mu < \mu_c$ is readily obtained from (24). The relation of $C(\mu)$ to η_1 is contained in (1), (22) and (25):

$$C(\mu) = \eta_1(\mu_W, \mu_b, \mu_c) m_c^2(\mu_c) b(\mu),$$

so that we can write down the final result now.

4.2.3 The Final Result for η_1 in Next-To-Leading Order

The coefficient η_1 in (1) reads in next-to-leading order:

$$\eta_1 = (\alpha(\mu_c))^{d_+^{(3)}} \sum_{i,j=+,-} \left(\frac{\alpha(\mu_b)}{\alpha(\mu_c)} \right)^{d_{ij}^{(4)}} \left(\frac{\alpha(\mu_W)}{\alpha(\mu_b)} \right)^{d_{ij}^{(5)}} \left\{ \tau_{ij} \left[1 + \frac{\alpha(\mu_c)}{4\pi} Z_+^{(3)} + \frac{\alpha(\mu_b) - \alpha(\mu_c)}{4\pi} Z_{ij}^{(4)} + \frac{\alpha(\mu_W) - \alpha(\mu_b)}{4\pi} Z_{ij}^{(5)} + \frac{\alpha(\mu_W)}{4\pi} b_{ij}(\mu_W) \right] + \frac{\alpha(\mu_c)}{4\pi} r_{ij}(\mu_c) \right\}. \quad (50)$$

The following table sums up in which equations the various quantities in (50) are defined:

$\alpha(\mu)$	$d_+^{(3)}$	$d_{ij}^{(f)}$	τ_{ij}	$Z_+^{(3)}$	$Z_{ij}^{(f)}$	b_{ij}	r_{ij}
(18)	(20)	(20)	(29)	(20)	(20)	(48)	(49), (44), (46)

Let us come back to the scale ambiguity at μ_c , which we had also discussed at the LL result by expanding $\eta_1(\mu_c)m_c^2(\mu_c)$ around $\mu_c = m_c^* = m_c(m_c)$ to order $\alpha \log(\mu_c^2/(m_c^*)^2)$ in (34). In the NLO expression (50) we encounter via r_{ij} additional contributions to the coefficient of $\alpha \log(\mu_c^2/(m_c^*)^2)$. They enter r_{ij} in (49) via $c_{LL}^{(ij)}$ given in (44). Consider for example the coefficient of the logarithm in $c_{LL}^{(--)}$. It reads

$$\tau_{--} 3(-3 - N) = \tau_{--} \left(\frac{\gamma_{--}^{(0)} - \gamma_+^{(0)}}{2} - \gamma_m^{(0)} \right)$$

and thereby cancels the corresponding coefficient in (34). The same holds for the other terms in the sum so that in the NLO result (50) the scale ambiguity at μ_c is removed to order α .

We have expanded (50) further to estimate the remaining dependence on μ_c . At order $\alpha^2 \log(\mu_c^2/(m_c^*)^2)$ we find a large contribution of the $(--)$ -term, which originates in the fact that the anomalous dimension of \mathcal{O}_{--} is negative and large in magnitude. In section 5 we will discuss the scale ambiguities numerically.

We close this section by mentioning another check of our result: If one switches off the running between μ_W and μ_c in (50) by expanding $[\alpha(\mu_W)/\alpha(\mu_b)]$ etc. around $\alpha(\mu_W)$, one must get the same result as by expanding η_2 calculated in [7] in m_t^2/M_W^2 and setting $m_t = m_c$. This is indeed the case.

5 Numerical Results

In this section we will point out the numerical impact of our NLO calculation on the value of η_1 and the $K_L - K_S$ mass difference. Special attention is paid to the dependence on the matching scales μ_c and μ_W .

The charm quark contribution to the $\Delta S = 2$ Hamiltonian was given in (4). Replacing the S function therein by its lowest nonvanishing order in the expansion with respect to m_c^2/M_W^2 leads to

$$\begin{aligned} H^c(\mu) &= \frac{G_F^2}{16\pi^2} \lambda_c^2 \cdot \eta_1(\mu_W, \mu_b, \mu_c) \cdot m_c^2(\mu_c) \cdot b(\mu) \cdot Q_{LL}(\mu) \\ &= \frac{G_F^2}{16\pi^2} \lambda_c^2 \cdot \eta_1^*(\mu_W, \mu_b, \mu_c) \cdot m_c^{*2} \cdot b(\mu) \cdot Q_{LL}(\mu) \end{aligned} \quad (51)$$

with

$$\begin{aligned} \eta_1^*(\mu_W, \mu_b, \mu_c) &= \frac{m_c^2(\mu_c)}{m_c^{*2}} \eta_1(\mu_W, \mu_b, \mu_c), \\ m_c^* &= m_c(m_c). \end{aligned} \quad (52)$$

$m_c(\mu_c)$ needed in (51) can be obtained from m_c^* by using the mass evolution equation (27).

$H^c(\mu)$ is directly related to physical observables and therefore must not depend on the scales μ_W, μ_b, μ_c . For this reason we have introduced η_1^* which multiplies only quantities which do not depend on these scales. η_1^* is only relevant for the discussion of the dependence on μ_c , since for $\mu_c = m_c^*$ one has $\eta_1 \equiv \eta_1^*$.

Let us recall the expression for η_1

$$\begin{aligned} \eta_1 &= (\alpha(\mu_c))^{d_+^{(3)}} \sum_{i,j=+,-} \left(\frac{\alpha(\mu_b)}{\alpha(\mu_c)} \right)^{d_{ij}^{(4)}} \left(\frac{\alpha(\mu_W)}{\alpha(\mu_b)} \right)^{d_{ij}^{(5)}} \left\{ \tau_{ij} \left[1 + \frac{\alpha(\mu_c)}{4\pi} Z_+^{(3)} + \frac{\alpha(\mu_b) - \alpha(\mu_c)}{4\pi} Z_{ij}^{(4)} \right. \right. \\ &\quad \left. \left. + \frac{\alpha(\mu_W) - \alpha(\mu_b)}{4\pi} Z_{ij}^{(5)} + \frac{\alpha(\mu_W)}{4\pi} b_{ij}(\mu_W) \right] + \frac{\alpha(\mu_c)}{4\pi} r_{ij}(\mu_c) \right\} \end{aligned} \quad (53)$$

and list its ingredients for the case $N = 3$:

$$d_+^{(3)} = \frac{2}{9}, \quad Z_+^{(3)} = -\frac{307}{162},$$

ij	++	+− = −+	−−
$d_{ij}^{(4)}$	$\frac{12}{25}$	$-\frac{6}{25}$	$-\frac{24}{25}$
$d_{ij}^{(5)}$	$\frac{12}{23}$	$-\frac{6}{23}$	$-\frac{24}{23}$
$Z_{ij}^{(4)}$	$-\frac{6719}{1875}$	$\frac{419}{3750}$	$\frac{7138}{1875}$
$Z_{ij}^{(5)}$	$-\frac{5165}{1587}$	$-\frac{631}{3174}$	$\frac{4534}{1587}$
τ_{ij}	$\frac{3}{2}$	$-\frac{1}{2}$	$\frac{1}{2}$
$r_{ij}(\mu_c)$	$-9 \log \frac{m_c^2}{\mu_c^2} - 5 - \frac{\pi^2}{6}$	$6 \log \frac{m_c^2}{\mu_c^2} - \frac{20}{3} + \pi^2 \frac{5}{18}$	$-9 \log \frac{m_c^2}{\mu_c^2} + \frac{35}{3} + \frac{\pi^2}{18}$
$b_{ij}(\mu_W)$	$4 \log \frac{\mu_W^2}{M_W^2} + \frac{22}{3}$	$-2 \log \frac{\mu_W^2}{M_W^2} - \frac{11}{3}$	$-8 \log \frac{\mu_W^2}{M_W^2} - \frac{44}{3}$

5.1 Numerical Results for η_1 and Δm_K

This section lists the numerical values for η_1 and the $K_L - K_S$ mass difference Δm_K . The scale ambiguities will be viewed at in sect. 5.2.

For our numerical estimates we will use $\Lambda_{\overline{\text{MS}}} = \Lambda_4$ and the following list of input parameters [26]:

$$\begin{aligned}
M_W &= 80 \text{ GeV}, & \mu_b &= m_b = 4.8 \text{ GeV}, \\
B_K &= 0.7, & m_K &= 0.498 \text{ GeV}, & f_K &= 0.161 \text{ GeV}, & (\Delta m)_K^{\text{EXP}} &= 3.522 \cdot 10^{-15} \text{ GeV}, \\
\text{Re}\lambda_c &= 0.215, & G_F &= 1.16639 \cdot 10^{-5} \text{ GeV}^{-2}.
\end{aligned} \tag{54}$$

In this section we will set the matching scales $\mu_c = m_c^*$ and $\mu_W = M_W$. Table 1 shows the LO and NLO result for η_1 for various values of m_c and $\Lambda_{\overline{\text{MS}}}$.

$\Lambda_{\overline{\text{MS}}}$	0.150		0.200		0.250		0.300		0.350	
m_c^*	LO	NLO	LO	NLO	LO	NLO	LO	NLO	LO	NLO
1.25	0.809	0.885	0.895	1.007	0.989	1.154	1.096	1.334	1.216	1.562
1.30	0.797	0.868	0.877	0.982	0.965	1.117	1.064	1.281	1.175	1.485
1.35	0.786	0.854	0.861	0.960	0.944	1.085	1.035	1.235	1.138	1.419
1.40	0.775	0.840	0.847	0.940	0.924	1.056	1.010	1.194	1.105	1.361
1.45	0.766	0.828	0.834	0.922	0.907	1.030	0.987	1.157	1.075	1.310
1.50	0.757	0.817	0.822	0.905	0.890	1.006	0.966	1.125	1.048	1.265
1.55	0.749	0.806	0.810	0.890	0.876	0.985	0.946	1.095	1.024	1.225

Table 1: η_1 to LO and NLO for different values of $\Lambda_4 = \Lambda_{\overline{\text{MS}}}$ and $\mu_c = m_c^*$ (both given in GeV).

From this table we see, that the NLO correction is positive and sizable. For a typical value of $\Lambda_{\overline{\text{MS}}} = 0.3 \text{ GeV}$ it amounts to about 20 percent of the LO result. The dependence of η_1 on $\Lambda_{\overline{\text{MS}}}$ turns out to be stronger when NLO effects are included. This can be seen from fig. 7, where we have taken $m_c^* = 1.4 \text{ GeV}$. Larger values of $\Lambda_{\overline{\text{MS}}}$ result in larger corrections and vice versa. The absolute value of η_1 decreases with increasing m_c .

Next, using (54), we calculate the contribution of H^c to the $K_L - K_S$ mass difference [8]

$$(\Delta m)_K^c = \frac{G_F^2}{6\pi^2} m_K f_K^2 B_K (\text{Re}\lambda_c)^2 m_c^{*2} \eta_1^* \tag{55}$$

with the result listed in table 2.

Since $(\Delta m)_K^c$ depends linearly on the B_K , the result can easily be rescaled to other values of this parameter.

Note that for $m_c^* = 1.4 \text{ GeV}$ and $\Lambda_{\overline{\text{MS}}} = 0.3 \text{ GeV}$ the contribution of H^c to $(\Delta m)_K^{\text{EXP}}$ is about 64 percent. If we also take into account the top quark contribution in $H^{\Delta S=2}$ (1),

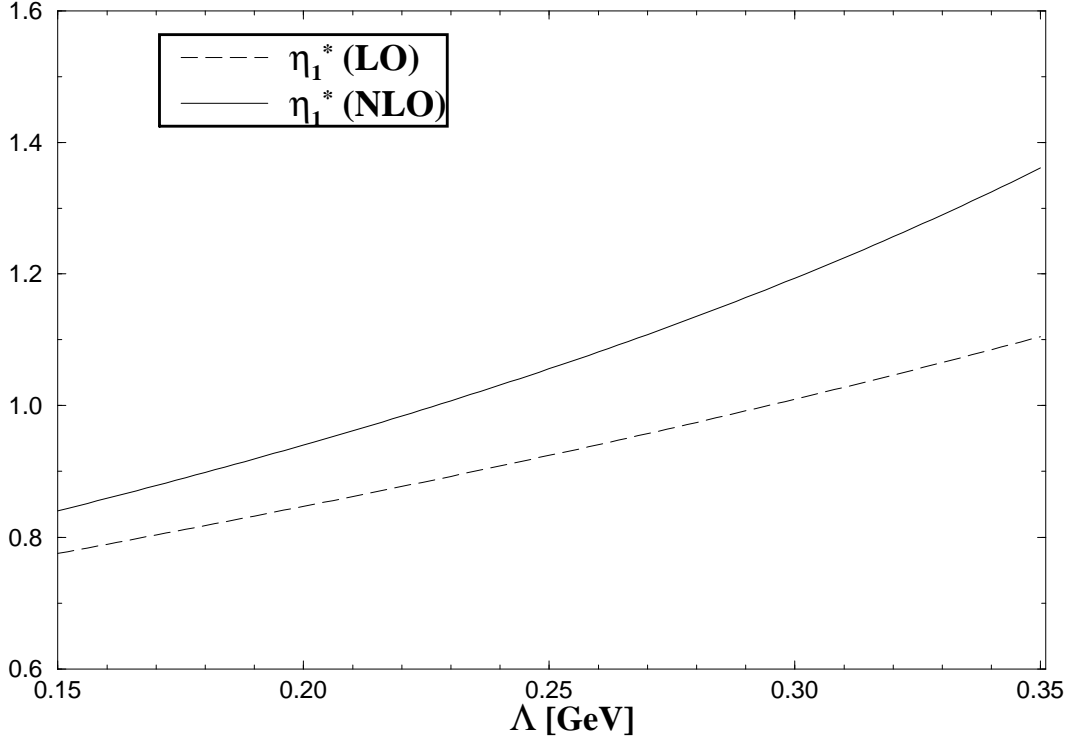


Figure 7: The dependence of η_1^* on $\Lambda_4 = \Lambda_{\overline{\text{MS}}}$.

which is about 6 percent, the complete short distance analysis reproduces about 70 percent of $(\Delta m)_K^{\text{EXP}}$.

Using vacuum insertion $B_K = 1$, the charm and top quark short distance contribution reproduces the full experimental mass difference, but [10, 11, 12, 13] favour a lower value for B_K .

5.2 Scale Dependences of η_1

Let us now discuss the dependence of η_1^* on the matching scale μ_c . We will fix the values of $m_c(\mu_c) = m_c^* = 1.4 \text{ GeV}$, $\mu_b = 4.8 \text{ GeV}$ and $\mu_W = M_W = 80 \text{ GeV}$. As can be seen from fig. 8 the scale dependence in the NLO calculation is reduced quite considerably compared to the LO result.

If we take as a reference value $\Lambda_{\overline{\text{MS}}} = 0.3 \text{ GeV}$, then varying μ_c from 1.1 to 1.7 GeV amounts to a change of 63% in the LO case and 34% in the NLO calculation:

$$\eta_1^* = 1.01 \begin{matrix} +0.42 \\ -0.21 \end{matrix} \quad \text{in LO} , \quad \eta_1^* = 1.19 \begin{matrix} +0.23 \\ -0.17 \end{matrix} \quad \text{in NLO} .$$

For $\Lambda_{\overline{\text{MS}}} = 0.2 \text{ GeV}$ the corresponding variations are 45% in LO and 20% in NLO:

$$\eta_1^* = 0.85 \begin{matrix} +0.24 \\ -0.13 \end{matrix} \quad \text{in LO} , \quad \eta_1^* = 0.94 \begin{matrix} +0.10 \\ -0.08 \end{matrix} \quad \text{in NLO} .$$

$\Lambda_{\overline{\text{MS}}}$	0.150		0.200		0.250		0.300		0.350	
m_c^*	Δm	$\frac{\Delta m}{\Delta m_{\text{EXP}}}$	Δm	$\frac{\Delta m}{\Delta m_{\text{EXP}}}$	Δm	$\frac{\Delta m}{\Delta m_{\text{EXP}}}$	Δm	$\frac{\Delta m}{\Delta m_{\text{EXP}}}$	Δm	$\frac{\Delta m}{\Delta m_{\text{EXP}}}$
1.25	1.327	0.377	1.510	0.429	1.730	0.491	2.000	0.568	2.342	0.665
1.30	1.408	0.400	1.593	0.452	1.812	0.514	2.078	0.590	2.409	0.684
1.35	1.493	0.424	1.679	0.477	1.897	0.539	2.159	0.613	2.481	0.705
1.40	1.580	0.449	1.768	0.502	1.986	0.564	2.245	0.637	2.560	0.727
1.45	1.670	0.474	1.860	0.528	2.078	0.590	2.335	0.663	2.643	0.751
1.50	1.763	0.501	1.955	0.555	2.173	0.617	2.428	0.689	2.731	0.776
1.55	1.859	0.528	2.052	0.583	2.271	0.645	2.525	0.717	2.824	0.802

Table 2: $(\Delta m)_K^c$ to NLO in units of 10^{-15} GeV for different values of $\Lambda_4 = \Lambda_{\overline{\text{MS}}}$ and $\mu_c = m_c^*$ (both given in GeV). $B_K = 0.7$.

The variation of μ_c between 1.1 and 1.7 GeV is quite conservative and may overestimate the ‘theoretical error’. Note, that setting $\mu_c \approx 1.25$ GeV in the LO expression already reproduces the NLO result for $\mu_c = 1.4$ GeV for all reasonable values of $\Lambda_{\overline{\text{MS}}}$.

We will further analyse the remaining scale setting ambiguity by looking at the individual contributions coming from the different terms in the sum in (53) as we already did analytically in sec. 4.2.3.

In fig. 9 one can easily see, that the $(++)$ and $(+-)$ contributions behave essentially flat as they should, but they contribute with opposite sign to η_1^* and therefore almost cancel in the sum. On the other hand the $(--)$ part carries a large residual scale dependence and is the largest of the three contributions.

Let us now continue with the discussion of residual scale dependences in η_1^* by varying the scale μ_W . We will fix $\mu_c = m_c^* = 1.4$ GeV, $\mu_b = 4.8$ GeV, $M_W = 80$ GeV. Also here — as in the case of μ_c discussed above — the scale dependence is reduced considerably by the inclusion of NLO effects. Taking $\Lambda_{\overline{\text{MS}}} = 0.3$ GeV and varying μ_W from 60 to 100 GeV we find a change of η_1^* by 7% in LO and 4% in NLO. This residual scale dependence therefore turns out to be small compared to the one found for μ_c .

η_1^* turns out to be very stable when varying the b -scale μ_b . Even if we neglect completely the effects from an effective 5 quark theory by setting $\mu_b = \mu_W$, therefore evolving from scale μ_W down to μ_c in an effective 4 quark theory, the error turns out to be of the order of 1 percent. This provides us with a simple and useful approximation for the numerical evaluation of η_1 .

$$\begin{aligned}
\eta_1 \approx (\alpha(\mu_c))^{d_+^{(3)}} \sum_{i,j=+,-} \left(\frac{\alpha(\mu_W)}{\alpha(\mu_c)} \right)^{d_{ij}^{(4)}} \left\{ \tau_{ij} \left[1 + \frac{\alpha(\mu_c)}{4\pi} Z_+^{(3)} + \frac{\alpha(\mu_W) - \alpha(\mu_c)}{4\pi} Z_{ij}^{(4)} \right. \right. \\
\left. \left. + \frac{\alpha(\mu_W)}{4\pi} b_{ij}(\mu_W) \right] + \frac{\alpha(\mu_c)}{4\pi} r_{ij}(\mu_c) \right\} \quad (56)
\end{aligned}$$

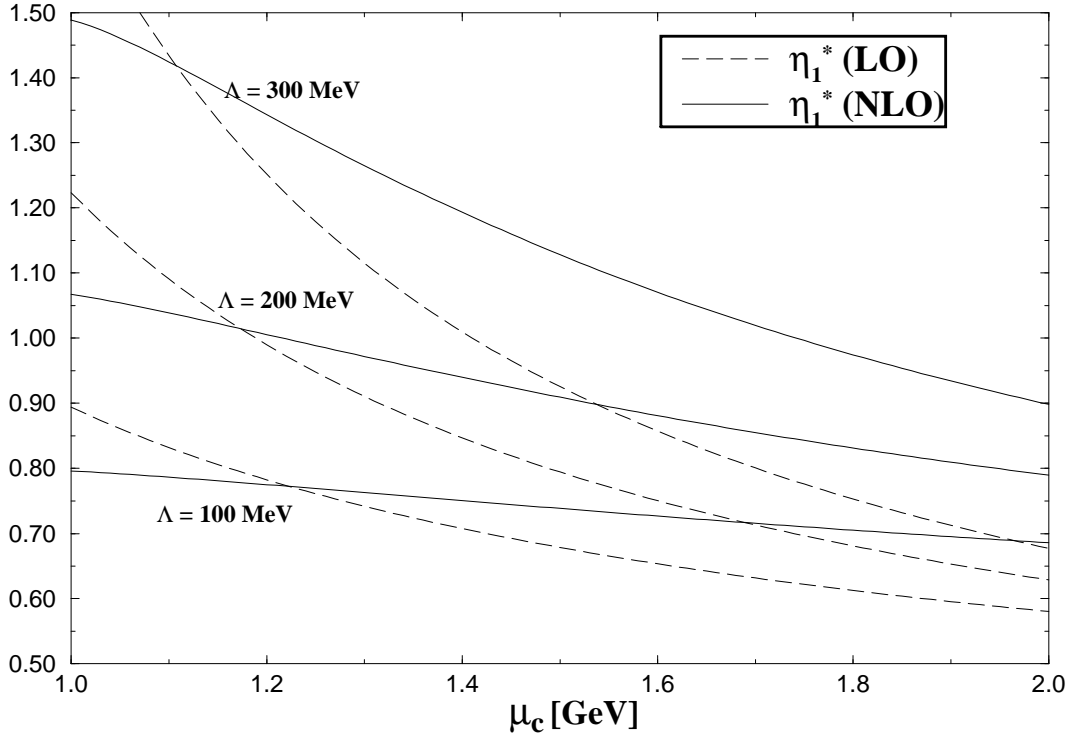


Figure 8: The dependence of η_1^* on the matching scale μ_c , where the c quark is removed from the theory for $\Lambda_{\overline{\text{MS}}} = 0.1, 0.2, 0.3$ GeV. $m_c^* = 1.4$ GeV has been kept fixed. The other scales have been chosen to be $\mu_b = 4.8$ GeV and $\mu_W = M_W = 80$ GeV .

6 Conclusions

In the present work we have calculated the complete next-to-leading order short distance QCD corrections to the coefficient η_1 of the effective $\Delta S = 2$ hamiltonian describing the $K^0-\overline{K}^0$ mixing. We have used dimensional regularization and the $\overline{\text{MS}}$ -scheme with anti-commuting γ_5 . Large logarithms have been summed by factorizing the Feynman amplitudes and applying the renormalization group evolution to the Wilson coefficients. To this end the renormalization of bilocal operators had to be studied in detail. We have explicitly proven that all Wilson coefficients involved in the calculation depend neither on the gluon gauge nor on the infrared regulators. We have further checked that the dependence of the leading order result on the renormalization scales is removed at NLO to order α .

The NLO short distance QCD corrections enhance η_1 by 20 % with respect to the LO result. The short distance part of the K_L-K_S mass difference is increased by the same amount, because it receives its dominant contribution from the first two quark generations. Finally the theoretical uncertainty due to the remaining dependence on the renormalization scale has been reduced by a factor of 2 compared to the LO result.

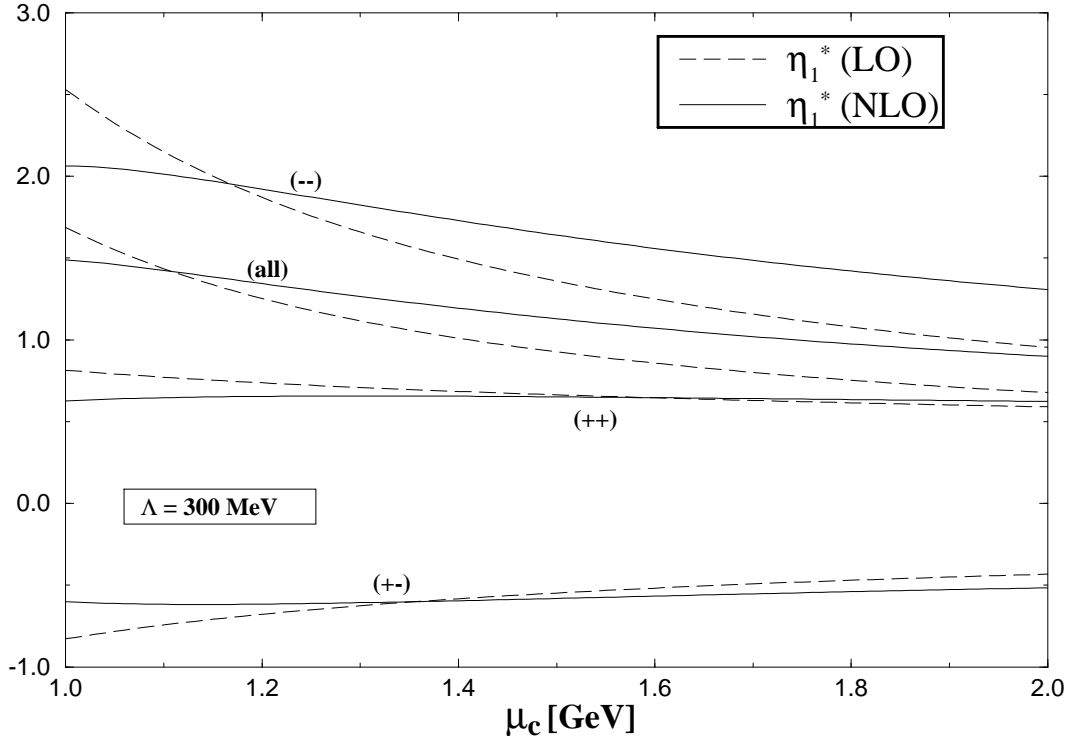


Figure 9: The dependence of the $(++)$, $(+-)$ and $(--)$ contributions to η_1^* on μ_c for $\Lambda_{\overline{\text{MS}}} = 0.3$ GeV. The line labeled by “all” is obtained by adding $(++) + 2(+-) + (--)$.

Acknowledgements

At first we would like to thank A. J. Buras for suggesting this project and for his permanent encouragement during our work. We are grateful to him and G. Buchalla for carefully reading the manuscript and appreciate many helpful discussions with them, M. E. Lautenbacher and M. Misiak.

A The Result for the Individual Diagrams

In this appendix we collect the results for the individual diagrams depicted in fig. 3 and fig. 4 including their QCD counterterms. The GIM mechanism has already been incorporated in the form $(c, c) - (u, c) - (c, u) + (u, u)$, where (k, l) denotes a diagram with internal k and l quarks. Then we get for the insertion of the bilocal operator \mathcal{O}^{ij}

$$\begin{aligned}
 D_0^{ij} &= -i \frac{1}{16\pi^2} m_c^2 D_0 \left(\mathcal{C}_0^{ij} \hat{1} + \tilde{\mathcal{C}}_0^{ij} \hat{1} \right), \\
 D_\ell^{ij} &= -i \frac{1}{16\pi^2} m_c^2 \frac{\alpha}{4\pi} \left(D_\ell^{\xi=0} + \xi D_\ell^{\text{gauge}} \right) \left(\mathcal{C}_\ell^{ij} \hat{1} + \tilde{\mathcal{C}}_\ell^{ij} \hat{1} \right), \quad \ell = 1, \dots, 7, \\
 D_8^{ij} &= 0,
 \end{aligned} \tag{57}$$

where \mathcal{C}_ℓ^{ij} and $\tilde{\mathcal{C}}_\ell^{ij}$ denote colour factors listed in table 3. The gauge independent part $D_\ell^{\xi=0}$ and the one proportional to the gluon gauge parameter D_ℓ^{gauge} read

$$\begin{aligned}
D_0 &= +\gamma_\mu L \otimes \gamma^\mu L [1] \\
D_1^{\xi=0} &= +\gamma_\mu R \otimes \gamma^\mu L \left[\frac{3 R_1(m_s^2, m_d^2) \frac{m_s m_d}{\mu^2}}{2} \right] \\
&\quad +\gamma_\mu L \otimes \gamma^\mu L \left[\frac{3}{2} \right] \\
D_1^{\text{gauge}} &= +\gamma_\mu R \otimes \gamma^\mu L \left[\frac{R_1(m_s^2, m_d^2) \frac{m_s m_d}{\mu^2}}{2} \right] \\
&\quad +\gamma_\mu L \otimes \gamma^\mu L \left[3 - \frac{\pi^2}{3} - S_1(m_s^2, m_d^2) + \log\left(\frac{m_c^2}{\mu^2}\right) \right] \\
D_2^{\xi=0} &= +R \otimes L \left[-3 R_1(m_s^2, m_d^2) \frac{m_s m_d}{\mu^2} \right] \\
&\quad +\gamma_\mu L \otimes \gamma^\mu L \left[-\frac{3}{2} \right] \\
D_2^{\text{gauge}} &= +R \otimes L \left[-\left(R_1(m_s^2, m_d^2) \frac{m_s m_d}{\mu^2} \right) \right] \\
&\quad +\gamma_\mu L \otimes \gamma^\mu L \left[1 - S_1(m_s^2, m_d^2) \right] \\
D_3^{\xi=0} &= +R \otimes R [-3] \\
&\quad +\gamma_\mu L \otimes \gamma^\mu L \left[-6 + 3 \log\left(\frac{m_s^2}{\mu^2}\right) + \pi^2 - 3 \log\left(\frac{m_c^2}{\mu^2}\right) \right] \\
&\quad +\sigma_{\mu\nu} \otimes \sigma^{\mu\nu} \left[\frac{3}{2} \right] \\
&\quad +\epsilon_{\mu\nu\eta\varphi} \sigma^{\mu\nu} \otimes \sigma^{\eta\varphi} \left[\frac{-3i}{4} \right] \\
D_3^{\text{gauge}} &= +R \otimes R [-1] \\
&\quad +\gamma_\mu L \otimes \gamma^\mu L \left[-2 + \log\left(\frac{m_s^2}{\mu^2}\right) + \frac{\pi^2}{3} - \log\left(\frac{m_c^2}{\mu^2}\right) \right] \\
&\quad +\sigma_{\mu\nu} \otimes \sigma^{\mu\nu} \left[\frac{1}{2} \right] \\
&\quad +\epsilon_{\mu\nu\eta\varphi} \sigma^{\mu\nu} \otimes \sigma^{\eta\varphi} \left[\frac{-i}{4} \right]
\end{aligned}$$

$$\begin{aligned}
D_4^{\xi=0} &= +\gamma_\mu L \otimes \gamma^\mu L \left[10 - \frac{2\pi^2}{3} \right] \\
D_4^{\text{gauge}} &= +\gamma_\mu L \otimes \gamma^\mu L \left[-4 + \frac{2\pi^2}{3} - 2 \log\left(\frac{m_c^2}{\mu^2}\right) \right] \\
D_5^{\xi=0} &= +\gamma_\mu L \otimes \gamma^\mu L \left[-2 - 3 \log\left(\frac{m_c^2}{\mu^2}\right) \right] \\
D_5^{\text{gauge}} &= +\gamma_\mu L \otimes \gamma^\mu L \left[2 - \frac{\pi^2}{3} + \log\left(\frac{m_c^2}{\mu^2}\right) \right] \\
D_6^{\xi=0} &= 0 \\
D_6^{\text{gauge}} &= +\gamma_\mu L \otimes \gamma^\mu L \left[-2 + \frac{\pi^2}{3} - \log\left(\frac{m_c^2}{\mu^2}\right) \right] \\
D_7^{\xi=0} &= +\gamma_\mu L \otimes \gamma^\mu L \left[-7 + 3 \log\left(\frac{m_c^2}{\mu^2}\right) \right] \\
D_7^{\text{gauge}} &= +\gamma_\mu L \otimes \gamma^\mu L \left[2 - \frac{\pi^2}{3} + \log\left(\frac{m_c^2}{\mu^2}\right) \right]
\end{aligned} \tag{58}$$

where the external spinors have been omitted. The mass singularities are contained in

$$\begin{aligned}
R_1(m_s^2, m_d^2) &= \mu^2 \frac{\log\left(\frac{m_s^2}{\mu^2}\right) - \log\left(\frac{m_d^2}{\mu^2}\right)}{m_s^2 - m_d^2}, \\
S_1(m_s^2, m_d^2) &= \frac{m_s^2 \log\left(\frac{m_s^2}{\mu^2}\right) - m_d^2 \log\left(\frac{m_d^2}{\mu^2}\right)}{m_s^2 - m_d^2}.
\end{aligned} \tag{59}$$

The expressions of diagrams generated from the generic ones in fig. 4 through a rotation by 180 degrees or a left–right–reflection are obtained from eq. (57) according to the following rules:

$$\begin{aligned}
D_1^{ij}: \gamma_\mu R \otimes \gamma^\mu L &\longrightarrow \gamma_\mu L \otimes \gamma^\mu R, \\
D_2^{ij}: R \otimes L &\longrightarrow L \otimes R, \\
D_3^{ij}: m_s &\longrightarrow m_d, \\
R \otimes R &\longrightarrow L \otimes L, \\
\varepsilon_{\mu\nu\eta\varphi} \sigma^{\mu\nu} \sigma^{\eta\varphi} &\longrightarrow -\varepsilon_{\mu\nu\eta\varphi} \sigma^{\mu\nu} \sigma^{\eta\varphi}.
\end{aligned}$$

To get the expressions for diagrams rotated by 90 degrees one has to apply a Fierz transformation.

ij	++		+-		-+		--	
ℓ	C_ℓ^{ij}	\tilde{C}_ℓ^{ij}	C_ℓ^{ij}	\tilde{C}_ℓ^{ij}	C_ℓ^{ij}	\tilde{C}_ℓ^{ij}	C_ℓ^{ij}	\tilde{C}_ℓ^{ij}
D ₀	1	$N+2$	1	$-N$	1	$-N$	1	$N-2$
D ₁	$\frac{2N^2+2N-1}{2N}$	$-\frac{N+2}{2N}$	$-\frac{1}{2N}$	$\frac{1}{2}$	$-\frac{1}{2N}$	$\frac{1}{2}$	$\frac{2N^2-2N-1}{2N}$	$-\frac{N+2}{2N}$
D ₂	$-\frac{1}{2N}$	$\frac{N^3+2N^2-2}{2N}$	$-\frac{1}{2N}$	$-\frac{N^2-2}{2}$	$-\frac{1}{2N}$	$-\frac{N^2-2}{2}$	$-\frac{1}{2N}$	$\frac{N^3-2N^2+2}{2N}$
D ₃	$\frac{N^2+2N-1}{2N}$	$-\frac{1}{N}$	$-\frac{N^2+1}{2N}$	1	$-\frac{N^2+1}{2N}$	1	$\frac{N^2-2N-1}{2N}$	$\frac{1}{N}$
D ₄	$-\frac{1}{2N}$	$\frac{N^3+2N^2-2}{2N}$	$-\frac{1}{2N}$	$-\frac{N^2-2}{2}$	$-\frac{1}{2N}$	$-\frac{N^2-2}{2}$	$-\frac{1}{2N}$	$\frac{N^3-2N^2+2}{2N}$
D ₅	$\frac{N^2-1}{2N}$	$\frac{N^3+2N^2-N-2}{2N}$	$\frac{N^2-1}{2N}$	$-\frac{N^2-1}{2}$	$\frac{N^2-1}{2N}$	$-\frac{N^2-1}{2}$	$\frac{N^2-1}{2N}$	$\frac{N^3-2N^2-N+2}{2N}$
D ₆	$\frac{N^2+N-1}{2N}$	$\frac{N^2-2}{2N}$	$\frac{N^2+N-1}{2N}$	$-\frac{N}{2}$	$\frac{N^2-N-1}{2N}$	$\frac{N}{2}$	$\frac{N^2-N-1}{2N}$	$-\frac{N^2-2}{2N}$
D ₇	$\frac{N-1}{2N}$	$\frac{N^2+N-2}{2N}$	$\frac{N-1}{2N}$	$-\frac{N-1}{2}$	$-\frac{N+1}{2N}$	$\frac{N+1}{2}$	$-\frac{N+1}{2N}$	$-\frac{N^2-N-2}{2N}$

Table 3: Color factors of the diagrams D_ℓ^{ij} , $\ell = 0, \dots, 7$

References

- [1] J. H. Christensen, J. W. Cronin, V. L. Fitch and R. Turlay, Phys. Rev. Lett. 13 (1964) 138.
J. H. Christensen, J. W. Cronin, V. L. Fitch and R. Turlay, Phys. Rev. 140B (1965) 74.
- [2] S. L. Glashow, J. Iliopoulos and L. Maiani, Phys. Rev. D2 (1970) 1285.
- [3] M. K. Gaillard and B. W. Lee, Phys. Rev. D10 (1974) 897.
- [4] M. I. Vysotskij, Sov. J. Nucl. Phys. 31 (1980) 797.
- [5] F. J. Gilman and M. B. Wise, Phys. Rev. D27 (1983) 1128.
- [6] T. Inami and C. S. Lim, Progr. Theor. Phys. 65 (1981) 297 [Erratum: 65 (1981) 1772].
- [7] A. J. Buras, M. Jamin and P. H. Weisz, Nucl. Phys. B347 (1990) 491.
- [8] A. J. Buras, W. Słominski and H. Steger, Nucl. Phys. B238 (1984) 529.
- [9] J.-M. Frère, W. A. Kaufman and Y.-P. Yao, Phys. Rev. D36 (1987) 809.
- [10] R. Gupta, G. W. Kilcup and R. S. Sharpe, Nucl. Phys. B (Proc. Suppl.) 26 (1992) 197.
M. B. Gavela et al., Nucl. Phys. B306 (1988) 138. C. Bernard and A. Soni, Nucl. Phys.

- B (Proc. Suppl.) 17 (1990) 495.
N. Ishizuka et al., Phys. Rev. Lett. 71 (1993) 24.
- [11] W. A. Bardeen, A. J. Buras and J.-M. Gérard, Phys. Lett. 211B (1988) 343.
- [12] R. Decker, in Proc. of the Ringberg Workshop on Hadronic Matrix Elements and Weak Decays,
Nucl. Phys. B (Proc. Suppl.) 7A (1989).
- [13] A. Pich and E. de Rafael, Nucl. Phys. B358 (1991) 311.
- [14] J. Bijnens, J.-M. Gérard and G. Klein, Phys. Lett. 257B (1991) 191.
- [15] A. J. Buras and P. H. Weisz, Nucl. Phys. B333 (1990) 66.
- [16] D. Kreimer Dissertation, Univ. Mainz 1992.
- [17] A. J. Buras, M. Jamin, M. E. Lautenbacher and P. H. Weisz,
Nucl. Phys. B370 (1992) 69.
- [18] G. Altarelli, G. Curci, G. Martinelli and S. Petrarca
Nucl. Phys. B187 (1981) 461.
- [19] E. Witten, Nucl. Phys. B122 (1977) 109.
- [20] C. Lee Nucl. Phys. B161 (1979) 171.
- [21] G. Buchalla and A. J. Buras, MPI-Ph/93-44 (hep-ph 9308272).
- [22] J. M. Flynn, Mod. Phys. Lett. A5 (1990) 877.
- [23] A. Datta, J. Fröhlich and E. A. Paschos, Z. Phys. C46 (1990) 63.
- [24] F. J. Gilman and M. B. Wise, Phys. Rev. D20 (1979) 2392.
- [25] M. Jamin and M. E. Lautenbacher, Comp. Phys. Comm. 74 (1993) 265.
- [26] Particle Data Group, Review of Particle Properties, Phys. Rev. D45, Part 2 (1992).